Research Square

Preprints are preliminary reports that have not undergone peer review.
They should not be considered conclusive, used to inform clinical practice,
or referenced by the media as validated information.

Molecular and Thermodynamic Evaluation of Ibuprofen and Mefenamic Acid Solubility in Choline Chloride–Propylene Glycol Deep Eutectic Solvent

Toyese OYEGOKE

oyegoketoyese@gmail.com

CAD Engineering of Processes & Reactive Interfaces (CEPRIs) Group, Chemical Engineering Department, Ahmadu Bello University, Faculty of Engineering

Umar Mogaji MUHAMMED

CAD Engineering of Processes & Reactive Interfaces (CEPRIs) Group, Chemical Engineering Department, Ahmadu Bello University, Faculty of Engineering

Research Article

Keywords: Drug delivery, Deep eutectic solvent, Drug solubility, Density functional theory, Molecular modeling, Solubility Strength, PM3, Ibuprofen, Mefenamic Acid

Posted Date: May 27th, 2026

DOI: https://doi.org/10.21203/rs.3.rs-8463299/v1

License: This work is licensed under a Creative Commons Attribution 4.0 International License.
Read Full License

Additional Declarations: No competing interests reported.

Molecular and Thermodynamic Evaluation of Ibuprofen and Mefenamic Acid Solubility in Choline Chloride–Propylene Glycol Deep Eutectic Solvent

Toyese Oyegoke* and Umar Mogaji Muhammed

CAD Engineering of Processes & Reactive Interfaces (CEPRIs) Group, Chemical Engineering Department, Ahmadu Bello University, Faculty of Engineering, Samaru, Zaria, Nigeria.

*Corresponding email: OyegokeToyese@gmail.com

Abstract

Understanding drug–solvent interactions at the molecular level is crucial for improving the solubility of poorly water-soluble pharmaceuticals. In this work, we computationally investigate the solubility behavior of ibuprofen (IBU) and mefenamic acid (MFA) in a choline chloride–propylene glycol (CHL–PG) deep eutectic solvent (DES) compared to water, using a hybrid approach that integrates PM3 semi-empirical conformer screening with ωB97X-D density functional theory calculations including dispersion and basis-set superposition error corrections. The DES is shown to form a stable dual hydrogen-bonded network (O–H and Cl–H), resulting in enhanced reactivity and favorable solute–solvent orbital interactions compared to aqueous media. Solubility strength (SS and solvation-corrected SScorr) and liquid-phase Gibbs free energy (ΔG) analyses reveal that IBU interacts favorably with the DES (SS = −0.75 eV; SScorr = −0.15 eV; ΔG = −0.147 eV), in agreement with experimental solubility (204.52 mg/g), whereas MFA exhibits weaker and non-spontaneous association (SS = −0.57 eV; SScorr = 0.46 eV; ΔG = 0.432 eV; LSS = 1.06 mg/g). Thermodynamic parameters further confirm the spontaneous, exothermic nature of IBU–DES solubilization and the comparatively unfavorable MFA–DES interaction. These results demonstrate the selective solubilization capability of CHL–PG DES and provide quantitative insights for rational design of DES-based drug delivery systems.

Keywords: Drug delivery, Deep eutectic solvent, Drug solubility, Density functional theory, Molecular modeling, Solubility Strength, PM3, Ibuprofen, Mefenamic Acid.

1 Introduction

Drug solubility remains a central challenge in pharmaceutical development and drug delivery. Many active pharmaceutical ingredients (APIs), particularly Biopharmaceutics Classification System (BCS) Class II drugs, exhibit poor aqueous solubility, which limits their dissolution rate, bioavailability, and therapeutic effectiveness [1–4]. Among these, Ibuprofen and Mefenamic acid are widely studied model compounds due to their low solubility and clinical relevance.

To address this limitation, significant research efforts have been directed toward the development of alternative solvent systems and formulation strategies. Recently, greener solvent technologies such as ionic liquids (ILs) [1] and deep eutectic solvents (DESs) [2, 3], have gained increasing attention as promising solubilizing media. DESs, formed by combining hydrogen bond acceptors and donors, exhibit unique physicochemical properties, including low volatility, tunability, and strong intermolecular interaction capabilities, making them suitable for enhancing drug solubility.

Several studies have demonstrated the effectiveness of these systems. Wahab et al. [4] reported that cholinium- and tetramethylammonium- based ionic liquids significantly enhanced the solubility of nonsteroidal anti-inflammatory drugs, including Ibuprofen (IBU), ketoprofen, and naproxen, with performance influenced by specific intermolecular interactions. Similarly, Boroomand et al. [5] showed that deep eutectic solvents based on choline chloride significantly improved the solubility of Artemisinin, with up to 310-fold enhancement compared to water.

In addition, a study in the literature [6] demonstrated that a choline chloride–propylene glycol (ChCl–PG) DES markedly improved the solubility of Metronidazole compared to aqueous systems. Fernandes et al. [7] further showed that solubility enhancement of Ibuprofen (IBU) in natural deep eutectic solvents (NADES) is highly solvent-dependent, with menthol-based systems exhibiting superior performance. Likewise, Nica et al. [8] improved the solubility of Mefenamic acid (MFA) through salt formation, demonstrating that disruption of intermolecular interactions enhances aqueous solubility.

Further studies have reinforced the potential of DES systems. Lamba et al. [9] reported that choline chloride–xylitol DES increased the solubility of Ibuprofen (IBU) by approximately 21-fold compared to water, while maintaining low toxicity. Nica et al. [10] also demonstrated that menthol-based DESs provide higher solubilization efficiency for both IBU and MFA, whereas sugar-based DESs offer tunability despite lower performance.

Many previous studies have experimentally highlighted the limitations associated with the poor aqueous solubility of ibuprofen. Some studies have focused on porous solid dispersions [11–14], while others have investigated the use of greener solvents [9, 10, 15] or hydrotropic agents [16, 17] to enhance its solubility. Most studies [9–14, 16–18] reported in the literature have primarily employed experimental approaches to improve ibuprofen solubility, with comparatively limited attention given to computational methods.

Despite these advances, existing studies remain largely experimental, with insufficient emphasis on computational investigations to elucidate drug–DES interactions at the molecular level, particularly for ibuprofen and mefenamic acid. A detailed understanding of hydrogen bonding, non-covalent interactions, and energetic contributions is essential for the rational design of solvent systems and accurate prediction of solubility behavior. Computational chemistry provides a powerful framework to address this gap by enabling molecular-level insights into drug–solvent interactions.

Therefore, the present study investigates the solubility enhancement of Ibuprofen and Mefenamic acid in a choline chloride–propylene glycol (CHL–PG) deep eutectic solvent in comparison with water. A hybrid computational approach was employed, incorporating the Parameterized Method 3 (PM3) [19–24] for geometry optimization, followed by ωB97X-D density functional theory calculations [25–27] using dual basis sets [28] with corrections for basis set superposition error (BSSE) [29] and dispersion interactions [30]. This approach provides detailed insight into interaction mechanisms and solubility enhancement.

2 Computational Methodology

2.1 Computational details

In the study of the ibuprofen (IBU) and mefenamic acid (MFA) drug solubility in a DES, we employed the use of Spartan molecular modeling package for the modeling and simulation of the solvent and its behavior with a computing device of 8 GB RAM, core i7 processor, processor speed of 2.60 GHz, and 256 GB SSD storage capacity. Following the strength of our computing resource, we deployed a hybrid approach of combining the use of semi-empirical with density functional theory (DFT) calculation method. In which, parameterized method 3 (PM3) [20–24] equilibrium conformer calculations were first carried out at an SCF tolerance of 10^9 to obtained most stable geometry for the model structures in the study. After which ωB97X-D hybrid [25–27] DFT calculations method with dual basis set (6-31G(D) [3-21G(*)]) was employed to improve on the accuracy of the energies obtained from the geometry optimization calculations, with the inclusion of dispersion [25, 30, 31] and basis set superposition error [28, 29, 32] correction for obtaining quality results useful for computing the drug solubility (evaluated as a function of the drug binding energy with the solvent) in the solvent in line with literature [33] which suggests the use of dual basis set as one of measure for correcting the basis set superposition error (BSSE) [28, 29] in the package. Other information on the study strategy, modelling of the molecules and the DES, including the interaction, solubility, thermodynamics, and other analysis are presented in the supplementary material (Section S4).

3 Results and Discussions

First, it is important to note that the preparation of the choline chloride–propylene glycol (CHL–PG) deep eutectic solvent (DES) and the computational procedures adopted for model generation have been thoroughly described in our earlier publication. Therefore, only a brief summary is provided here, while full methodological details, including DES composition, structural optimization procedures, and computational parameters, which are presented in the Supplementary Information (SI). In summary, the DES was constructed by combining CHL as the hydrogen bond acceptor (HBA) with PG as the hydrogen bond donor (HBD), followed by full quantum-chemical optimization of each component and their associated complexes for the DES (CHL–PG). Multiple potential interaction sites were systematically evaluated to determine favorable hydrogen-bonding pathways that could support DES formation, which is presented in the SI and our related literature [34]. The molecular models were validated through comparison of the simulated infrared spectra with corresponding experimental data reported in literature [35]. With this validated model established, the subsequent sections present the predicted molecular properties, formation pathways, relative stabilities, and relevance of the DES (CHL–PG) for enhancing the solubility of selected drugs (IBU and MFA).

3.1 Modeling the most stable interaction pathways for DES formation

In Table 1, we summarize the single-site hydrogen-bonding pathways (which includes, H_3C-HOCH, H_2C-HCOH, H_2CO-$HOCH_2$, NCl-$HOCH_2$, ClN-HCH, and OHC-HCH) evaluated for DES (CHL–PG) formation, comparing the unbonded complex (that is, one with no modeled bonds) with six possible interaction routes (as reported in SI).

Table 1: Most stable interactions across the different single hydrogen bonding interaction DES formation pathways

Sites		*Energy (eV)*	*Formation Energy (eV)*
CHL-PG (with no modeled bonds)		-28801.59	-0.96
HBA Sites	*HBD Sites*	-	-
H_3C	HOCH	-28801.66	-1.04
H_2C	HCOH	-28801.71	-1.08
H_2CO	$HOCH_2$	-28802.14	-1.51
NCl	$HOCH_2$	-28801.49	-0.86
ClN	HCH	-28801.49	-0.86
OHC	HCH	-28802.03	-1.40
Single site	Overall most stable	-28802.14	-1.51 [O-H(H_2CO-$HOCH_2$) = 1.83 Å, Cl-H(NCl-HOCH) = 2.43 Å]
Double sites	Dual hydrogen bonding	-28802.13	-1.50 [O-H(H_2CO-$HOCH_2$) = 1.83 Å, Cl-H(NCl-HOCH) = 2.44 Å]

Among these sets of formation pathways (as shown in Table 1) explored in our study, the H_2CO–$HOCH_2$ pathway was identified as the most stable, exhibiting the lowest formation energy (−1.51 eV). This strong stabilization indicates spontaneous complex formation driven by a robust hydrogen bond between the oxygen atom of CHL's H_2CO- group and the hydrogen atom of PG's -$HOCH_2$ group, which was due to the highly negative reaction or formation energy obtained for its pathway compared to other pathways in line with the literature [36, 37]. The result underscores the key role of hydroxyl and ether functionalities in promoting strong hydrogen bonding or electrostatic interactions and establishing the most favorable single-site route for DES formation. Though, the optimized geometry in Figure 3 later reveal that the most favorable route do not only engaged one interaction route, but instead employed the use of two different interaction routes (Cl-H and O-H).

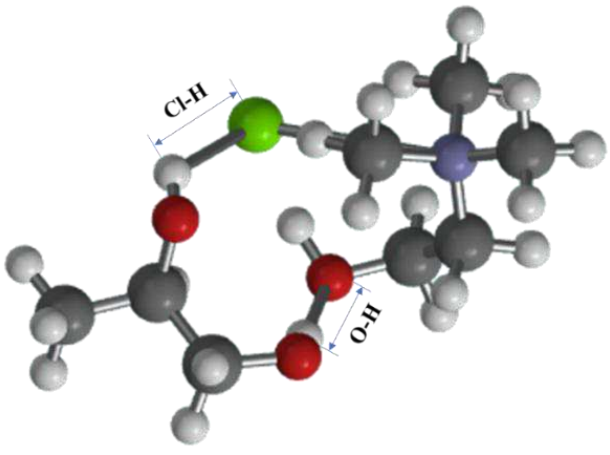

Figure 3: The most stable geometric structure of the formed DES via dual hydrogen bonding interaction H_2CO-$HOCH_2$ and NCl-HOCH (Cl-H = 2.44 Å, O-H = 1.83 Å).

To determine whether cooperative interactions could further enhance stability, a dual-site mechanism, as shown in Figure 3, was explored by combining the most favorable single-site interaction (H_2CO–$HOCH_2$) with a simultaneous NCl–HOCH hydrogen bond. The results presented in Table 1 confirm that this dual-interaction pathway exhibits formation energies (−1.50 to −1.51 eV) and bond lengths nearly identical to those of the most stable single-site

pathway (with optimized geometry that equally shows dual-site interaction in Appendix S3 of the SI), demonstrating that both mechanisms yield essentially the same optimized structure. This close agreement indicates that CHL–PG DES formation is governed by a stable dual hydrogen-bonding arrangement. Accordingly, subsequent analyses in this study adopt the optimized geometry in Figure 3, which represents the dual hydrogen-bonding interactions at H_2CO–$HOCH_2$ (O–H) and NCl–HOCH (Cl–H), as detailed extensively in the SI of this draft.

3.2 Analysis of the molecular interaction of DES and water with the drugs

The molecular properties of the DES (CHL–PG), water, ibuprofen (IBU), and mefenamic acid (MFA) are presented in Figure 4 and Table 2, providing insight into their electronic structures and reactivity profiles relevant to solubility enhancement.

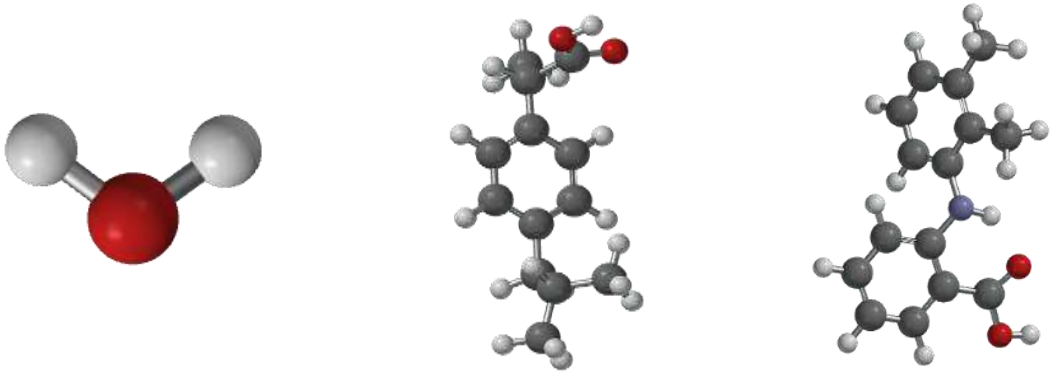

Figure 4: Optimized geometry of water, ibuprofen (IBU) and mefenamic acid (MFA)

The energy band gap (EGap) is a key indicator of molecular stability and chemical reactivity. The DES exhibited an EGap of 11.05 eV, lower than that of water (14.56 eV) but higher than those of IBU (9.96 eV) and MFA (7.76 eV). This suggests that the DES is more reactive than water, consistent with literature reports [38–40], and therefore more capable of engaging in favorable solute–solvent interactions.

Table 2: Molecular properties of the DES and water for IBU and MFA solubility.

Specie	*E HOMO (eV)*	*E LUMO (eV)*	*EGap (eV)*	*Interaction Energy Band Gap (IEG) (eV)*					
				ibuHOMO	*ibuLUMO*	*minIEG*	*mfaHOMO*	*mfaLUMO*	*minIEG*
IBU	-9.10	0.85	9.96	9.96	9.96	9.96	-	-	-
MFA	-8.13	-0.37	7.76	-	-	-	7.76	7.76	7.76
DES	-8.67	2.37	11.05	11.48	9.52	9.52	10.50	8.30	8.30
H_2O	-10.35	4.21	14.56	13.31	11.20	11.20	12.34	9.98	9.98

The interaction energy band gap (IEG) further clarifies solvent–drug interaction strength. Both IBU and MFA showed lower IEG values with the DES compared to water, indicating stronger and more feasible interactions. In each case, the most favorable orbital overlap occurred between the solvent EHOMO and the drug ELUMO, establishing the drugs as electron acceptors (electrophilic species) and the solvents as electron donors (nucleophilic species). This agrees with established theoretical expectations in the literature [39, 40]. The lowest IEG values of 9.52 eV for IBU and 8.30 eV for MFA were obtained with the DES, whereas water showed significantly higher values (11.20 eV and 9.98 eV), reflecting weaker interactions. Overall, these results demonstrate that the CHL–PG DES, particularly in its dual-site configuration, offers a more suitable electronic environment for enhancing IBU and MFA solubility relative to conventional solvents such as water.

3.3 Evaluation of the solubility of the drugs in water

Five possible interaction pathways governing the dissolution of the drugs in water were evaluated, as presented in Table 3 for IBU and MFA. These pathways were modeled to identify the most energetically favorable drug–solvent mechanism or configuration. The computed electronic energies and corresponding solubility indicators for each pathway are summarized in Tables.

Table 3: Solubility Strength (SS) Calculation as a function of Binding Energy via IBU and MFA in water interaction

Species		*Mol. Wt. (amu)*	*E (eV)*	*SS (eV)*	*Species*		*Mol. Wt. (amu)*	*E (eV)*	*SS (eV)*
H_2O		18.02	-2078.59	-	H_2O		18.02	-2078.59	-
IBU		206.29	-17864.02	-	MFA		241.29	-21377.18	-
IBU–H_2O	No bond	224.30	-19942.95	-0.34	MFA–H_2O	No bond	259.31	-23456.02	-0.25
	HO-HOH	224.30	-19942.95	-0.34		OH-OH_2	259.31	-23456.39	-0.62
	COH-OH_2	224.30	-19943.15	-0.54		CO-HOH	259.31	-23455.81	-0.04
	HOC-OH_2	224.30	-19942.86	-0.26		HN-HOH	259.31	-23456.06	-0.30
	HOC-HOH	224.30	-19942.86	-0.26		HN- OH_2	259.31	-23455.83	-0.06
Comp	COH-OH_2	-	-	-0.54	Comp	OH-OH_2	-	-	-0.62
Expt	Ref: [41, 42]	-	-	21 mg/l @ 25 °C	Expt	Ref: [43, 44]	-	0.0041g /100ml @ 25 °C	41 mg/l @ 25 °C

Our analysis of the results presented in Table 3 for the solubility of IBU in water shows that the COH–OH_2 interaction pathway exhibits the most negative binding energy (–0.54 eV) among all evaluated routes. According to established literature [45–47], pathways with stronger (more negative) binding energies are more likely to promote IBU–water interactions, thereby enhancing the solubility of the drug in aqueous media.

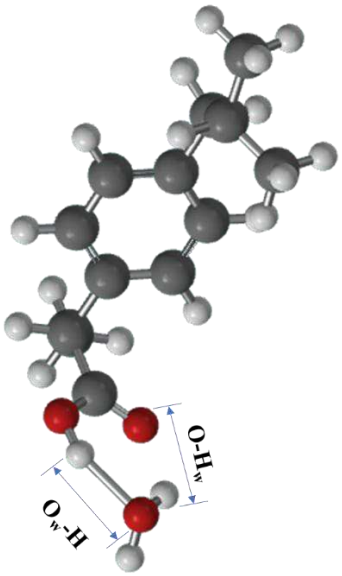

Figure 5: Optimized geometry structure of most negative IBU-H_2O interaction (O-Hw = 1.82 Å, Ow-H = 1.81 Å).

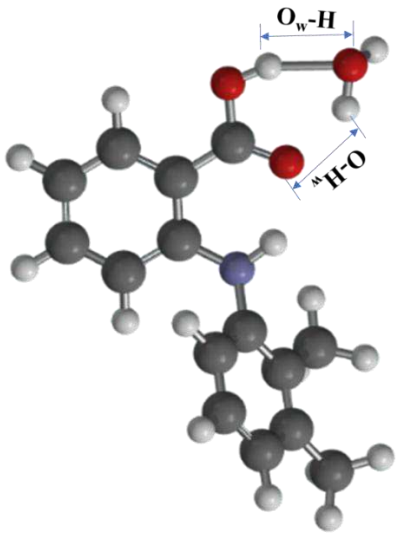

Figure 6: Optimized geometry structure of most negative MFA-H_2O interaction (O-Hw = 1.82 Å, Ow-H = 1.78 Å).

Figure 5 presents the optimized geometry for the most stable and favorable interaction route (COH–OH_2) between IBU and water. Further examination of the binding energy in Table 3, together with the optimized geometry in Figure 5, confirms that the most feasible solubility mechanism involves dual hydrogen-bonding interactions. This is supported by the presence of two hydrogen-bond distances (O–Hw = 1.82 Å and Ow–H = 1.81 Å), indicating that two simultaneous hydrogen bonds contribute to the stabilization and dissolution of IBU in water.

Further analysis of the MFA–water interaction pathways in Table 3 shows that the OH–OH_2 pathway exhibits the most negative binding energy (–0.62 eV) among all pathways evaluated, confirming it as the most stable and favorable interaction route between MFA and H_2O (Figure 6). This observation is consistent with literature reports [32, 36, 48–51], which indicate that more negative binding energies correspond to stronger intermolecular interactions.

The MFA–water interaction strength was also found to be higher than that of IBU–water by approximately 0.08 eV. These findings are in agreement with experimental reports [41–44], which indicate that IBU [41] is less soluble in water than MFA [44], despite both drugs generally exhibiting poor aqueous solubility. The optimized geometry shown in Figure 6 further supports this observation, revealing a dual hydrogen-bonding interaction pathway with shorter bond distances for the MFA–water system compared to the IBU–water system. These shorter bond distances likely contribute to the stronger interactions and enhanced solubility observed for MFA relative to IBU in aqueous media.

3.4 Evaluation of the solubility of the drugs in the DES

In contrast to conventional solvents like water, analyzed in the previous section, we further explored the potential of the DES (CHL-PG), which is widely recognized as an environmentally friendly, green solvent with numerous applications [2, 52–55], including enhancing drug solubility for drug delivery. The results of the modeled interactions of IBU and MFA with the DES are presented in Table 4.

Table 4: Solubility Strength (SS) Calculation as a function of Binding Energy via IBU and MFA in DES interaction.

Species		*Mol. Wt. (amu)*	*E (eV)*	*SS (eV)*	*Species*		*Mol. Wt (amu)*	*E (eV)*	*SS (eV)*
DES		215.72	-28802.13	-	DES		215.72	-28802.13	-
IBU		206.29	-17864.02	-	MFA		241.29	-21377.18	-
IBU–DES	No bond	422.01	-46666.07	0.08	MFA–DES	No bond	457.01	-50178.45	0.85
	CO-HOH	422.01	-46666.73	-0.59		COH-OH	457.01	-50179.20	0.11
	CO-HCOH	422.01	-46666.41	-0.27		COH-ClN	457.01	-50179.58	-0.27
	OH-ClN	422.01	-46666.89	-0.75		C_3H- ClN	457.01	-50179.29	0.01
	CCH-OH	422.01	-46666.59	-0.45		H_2CH-CH_2OH	457.01	-50179.88	-0.57
Comp	OH-ClN	-	-	-0.75	Comp	H_2CH-CH_2OH	-	-	-0.57
Expt	Ref: [10]	-	-	204.52 mg/g	Expt	Ref: [10]	-	-	1.06 mg/g

Using the electronic energy (E) and solubility strength (SS), we evaluated the different IBU dissolution pathways presented in Table 4. The pathway with the most negative electronic energy corresponds to the most stable configuration, while the most negative solubility strength (–0.75 eV) identifies the most feasible dissolution mechanism. This pathway involves the OH–ClN interaction pair between IBU and the DES, as shown in Figure 7. This indicates that IBU dissolves most favorably in the DES through the hydrogen of its hydroxyl group (OH–) interacting with the chloride site (–ClN) of the DES, suggesting that the interaction is strongly influenced by electrostatic attraction between IBU's hydroxyl group and the DES chlorine atom, since unlike charged point tend to exhibit an electrostatic interaction in accordance with the existing works [56–59] in the literature.

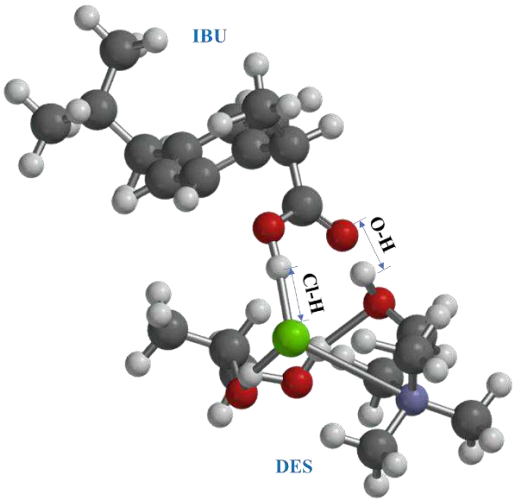

Figure 7: Optimized geometry structure of most negative IBU-DES interaction (O-H = 1.79 Å, Cl-H = 1.75 Å).

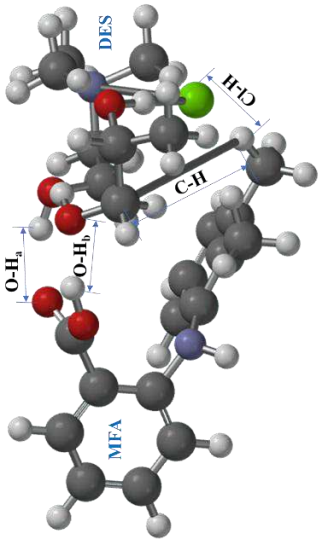

Figure 8: Optimized geometry structure of most negative MFA-DES interaction (O-H_b = 1.78Å, O-H_a = 1.80Å, Cl-H = 2.55Å, C-H = 5.45Å).

Similarly, the solubility of MFA in the DES was evaluated by examining various possible dissolution pathways, as presented in Table 4. The analysis confirms that the most feasible interaction pathway occurs between the H_2CH group of the MFA and the $–CH_2OH$ group of the DES, as shown in Figure 8. This pathway exhibits the most negative solubility strength (–0.57 eV), indicating the strongest and most favorable interaction for MFA dissolution in the DES.

3.5 Comparative analysis of the IBU and MFA in the different solvents studied

In this section, it should be noted that SS represents the solubility strength computed under vacuum conditions, whereas SScorr corresponds to the solubility strength calculated in the presence of a solvent environment (aqueous phase). Thus, SS reflects intrinsic interaction strength in the absence of solvent effects, while SScorr provides a more realistic description by accounting for solvent-mediated interactions. In Table 5, the most feasible interaction pathways (or sites) responsible for the solubility strength of the drugs (IBU and MFA) in both water and DES (CHL-PG) systems are summarized. The solubility strength values were computed based on the most energetically favorable interactions identified in the preceding sections.

The predicted solubility trend in water, SS for IBU (−0.54 eV) < SS for MFA (−0.62 eV), shows good agreement with experimental literature [41–44]. Reported solubility values in the literature [41, 44] indicate that IBU (0.021 mg/g at 25 °C) exhibits lower solubility compared to MFA (0.04 mg/g at 25 °C), confirming weaker interaction of IBU with water relative to MFA.

Table 5: Summary of drug solubility in DES and water.

Drug	*Solvent*	*Interactions Site*	*E (eV)*	*Ecorr. (eV)*	*ΔEerr (eV)*	*SS (eV)*	*SScorr. (eV)*	*ΔSSerr (eV)*	*LSS (mg/g)*	*Ref. LSS*
IBU	H_2O	COH-OH_2	-19943.15	-19949.69	-6.54	-0.54	-0.31	0.23	0.02	[41]
	DES	OH-ClN	-46666.89	-46678.04	-11.15	-0.75	-0.15	0.60	204.52	[10]
MFA	H_2O	OH-OH_2	-23456.39	-23464.34	-7.95	-0.62	-0.31	0.31	0.04	[44]
	DES	H_2CH-CH_2OH	-50179.88	-50192.09	-12.21	-0.57	0.46	1.03	1.06	[10]
	Correlation Coefficient of (LSS/x)		-0.50	-0.50	-0.43	-0.93	-0.13	0.11	1.00	Calc

Compared with IBU, MFA exhibits a weaker dissolution tendency in the DES. IBU shows stronger solubility strength (SS = −0.75 eV, SScorr = −0.15 eV), whereas the MFA–DES

interaction is less favorable (SS = −0.57 eV, SScorr = 0.46 eV). This observation is consistent with experimental literature [10] values (204.52 mg/g for IBU and 1.06 mg/g for MFA). Notably, the SS values, which include solvent effects, provide a better basis for comparison with experimental solubility data. This contrast is further supported by the shorter bond distances observed for IBU (Figure 7), which promote stronger intermolecular interactions and enhanced solubility. In contrast, the longer bond distances observed for MFA (Figure 8) indicate weaker interactions. This is consistent with literature [60, 61] that stronger binding interactions are associated with shorter interaction distances.

Further analysis of Table 5 reveals that MFA exhibits lower solubility in the DES (SS = −0.57 eV, SScorr = 0.46 eV) compared to water (SS = −0.62 eV, SScorr = −0.313 eV). In contrast, IBU shows improved solubility in the DES (SS = −0.75 eV, SScorr = −0.15 eV) relative to water (SS = −0.54 eV, SScorr = −0.307 eV), demonstrating the superior dissolution performance of the DES for IBU. Overall, the results indicate that the DES would more favorably enhance the solubility of IBU, whereas MFA does not benefit similarly due to its weaker solubility in the DES compared with the conventional solvent (water).

In a nutshell, the comparative analysis demonstrates that the DES (CHL–PG) provides a significantly more favorable solvation environment for IBU than for MFA. The stronger IBU–DES interaction, reflected in both lower solubility strength values and shorter hydrogen-bond distances, indicates enhanced compatibility between the DES components and the functional groups of IBU. In contrast, MFA shows reduced solubility in the DES relative to water, suggesting less effective molecular recognition within the DES matrix. These findings highlight the selective solubilization capability of the DES (CHL–PG) and emphasize that its solubility-enhancing potential is drug-dependent.

3.6 Thermodynamic Analysis of IBU–DES and MFA–DES Interactions

The thermodynamic parameters of the IBU–DES and MFA–DES systems at 300 K were evaluated using the non-volatile liquid-phase correction approximation, and the results are summarized in Table 6. These parameters provide direct insight into the solute–DES interactions under conditions relevant to solubility, while gas-phase computations were used solely to obtain the liquid-phase corrected values and are provided in the Supplementary Material (Section S5).

Table 6: Thermodynamic analysis of the drugs with DES at 300K.

Solubility	*Enthalpy* $\Delta H = dHliq$ *(eV)*	*Entropy* $\Delta S = dSliq$ *(eV/K)*	*Gibb Free Energy* $\Delta G = dGliq$ *(eV)*	*Lab Experiment*	
				LSS (mg/g)	*LSS Ref*
DES+IBU	-0.3942	-0.000825	-0.1466	204.52	[10]
DES+MFA	0.1794	-0.000841	0.4316	1.06	[10]
Corr. Coef. R-value	-1	na	-1	1	Calc

In the liquid phase, the DES+IBU system exhibits a negative enthalpy (ΔH = −0.3942 eV), indicating an exothermic [56] interaction. This suggests strong and favorable interactions between IBU and the DES components, consistent with the high experimental solubility (204.52 mg/g). In contrast, the DES+MFA system shows a positive enthalpy (ΔH = 0.1794 eV), indicating an endothermic process and weaker interactions, which corresponds to its very low solubility (1.06 mg/g) in accordance with the literature report [10].

The entropy changes for both systems are slightly negative (ΔS = −0.000825 eV/K for DES+IBU and −0.000841 eV/K for DES+MFA), reflecting increased structural ordering [56, 62, 63] upon solute incorporation into the DES. This is likely due to the formation of structured solvation shells and specific intermolecular interactions, such as hydrogen bonding and van der Waals forces. The slightly smaller magnitude of entropy reduction for IBU suggests that it is more efficiently accommodated within the DES network than MFA.

Gibbs free energy, which integrates both enthalpic and entropic contributions, further highlights the thermodynamic favorability [56, 62, 63] of the interactions. The DES+IBU system has a negative ΔG (−0.1466 eV), indicating spontaneous solubilization under liquid-phase conditions, in excellent agreement with experimental observations [10]. Conversely, DES+MFA shows a positive ΔG (0.4316 eV), confirming that solubilization is non-spontaneous, consistent with its low experimental solubility.

Overall, the liquid-phase thermodynamic analysis clearly demonstrates that IBU interacts more favorably with the DES than MFA. The correlation between negative ΔG and high experimental solubility [10] underscores the predictive value of these parameters for solute–DES compatibility. The R-values further support this relationship, with ΔG inversely correlating with solubility, confirming the reliability of the liquid-phase corrected approach for describing nonvolatile systems.

4 Conclusions and Recommendations

The solubility of ibuprofen (IBU) and mefenamic acid (MFA) in choline chloride–propylene glycol (CHL–PG) deep eutectic solvent (DES) was systematically investigated using a hybrid computational approach combining PM3 semi-empirical and ωB97X-D DFT methods. The DES forms a stable hydrogen-bonded network with dual interaction sites (O–H and Cl–H), providing enhanced structural stability and favorable solvation. IBU exhibits significantly higher solubility in the DES (SS = −0.75 eV, SScorr = −0.15 eV; ΔG = −0.1466 eV; LSS = 204.52 mg/g) compared to MFA (SS = −0.57 eV, SScorr = 0.46 eV; ΔG = 0.4316 eV; LSS = 1.06 mg/g), which was consistent with the experimental data.

Thermodynamic analysis shows that IBU–DES interactions are exothermic (ΔH = −0.3942 eV) with slightly negative entropy (ΔS = −0.000825 eV/K), whereas MFA–DES interactions are endothermic (ΔH = 0.1794 eV), reflecting weaker affinity. In overall, the CHL–PG DES effectively enhances IBU solubility while providing limited benefit for MFA. The results underline the predictive value of liquid-phase thermodynamic parameters for assessing solute–DES compatibility and suggest that alternative DES compositions or conditions may be required for drugs with weaker interactions. Future studies exploring temperature, solute concentration, and DES formulation variations are recommended to optimize solubility and support sustainable drug delivery applications.

5 Funding

The project was not funded.

6 CRediT authorship contribution statement

T.O.: Conceptualization, Formal analysis, Investigation, Software, Supervision, Methodology, Resources, Validation, Visualization, Writing – original draft, Writing – review & editing.

U.M.M.: Formal analysis, Investigation, Software, Resources, Validation, Writing – review & editing.

7 Declaration of generative AI in scientific writing

During the preparation of this work, the author(s) used Grammarly and OpenAI to improve readability and language, eliminating grammatical or language-related errors. After utilizing these tools/services, the author(s) reviewed and edited the content as necessary and assumed full responsibility for the publication's content.

8 Conflict of Interest

The authors do declare no any conflict of interest in the report.

9 Supplementary materials

There is one in the attachment.

10 Acknowledgement

The authors wish to acknowledge the support of the Wavefunction Inc. USA for the provision of both trial and discounted license for their Spartan Modeling packages which was employed in project. In addition, we do appreciate the motivational support of the other members of CEPRIs Group Lab and other member of Pencil Team.

11 Data availability

All data employed in the study are provided therein the manuscript and supplementary material.

12 References

1. Chen Y, Mu T (2021) Revisiting greenness of ionic liquids and deep eutectic solvents. Green Chemical Engineering 2:174–186. https://doi.org/10.1016/J.GCE.2021.01.004

2. Hou YC, Yao CF, Wu WZ (2018) Deep eutectic solvents: Green solvents for separation applications. Wuli Huaxue Xuebao/ Acta Physico - Chimica Sinica 34:873–885. https://doi.org/10.3866/PKU.WHXB201802062

3. Omar KA, Sadeghi R (2023) Database of deep eutectic solvents and their physical properties: A review. J Mol Liq 384:121899. https://doi.org/10.1016/J.MOLLIQ.2023.121899

4. Wahab OO, Govender KK, Govender PP (2025) Computational study of hydroxides of cholinium and tetramethylammonium derivatives as biofriendly ionic liquids for improved drug solubility and delivery. J Mol Liq 439:128954. https://doi.org/10.1016/J.MOLLIQ.2025.128954

5. Boroomand S, Mohammad-Aghaie D, Mohammadpour F (2025) Molecular dynamics and DFT analysis of artemisinin solubility in acidic deep eutectic solvents: Implications for cancer drug delivery. J Mol Liq 435:128050. https://doi.org/10.1016/J.MOLLIQ.2025.128050

6. Muhammed UM, Oyegoke T (2025) Enhancing the Solubility of Metronidazole Using Deep Eutectic Solvents: A Computational Insight Into a Green Formulation Strategy

7. Fernandes CC, Paiva A, Haghbakhsh R, Duarte ARC (2025) Understanding the Solubility behaviour of Ibuprofen and Xylitol in Natural Deep Eutectic Systems through Hansen Solubility Parameters and Physicochemical Properties. J Mol Liq 428:127544. https://doi.org/10.1016/J.MOLLIQ.2025.127544

8. Nica MA, Anuța V, Nicolae CA, Popa L, Ghica MV, Cocoș FI, Dinu-Pîrvu CE (2024) Exploring Deep Eutectic Solvents as Pharmaceutical Excipients: Enhancing the Solubility of Ibuprofen and Mefenamic Acid. Pharmaceuticals 17:1316. https://doi.org/10.3390/PH17101316/S1

9. Lomba L, Garralaga MP, Werner Á, Giner B, Baptista PM, Sánchez-Romero N (2023) Ibuprofen solubility and cytotoxic study of deep eutectic solvents formed by xylitol, choline chloride and water. J Drug Deliv Sci Technol 82:104327. https://doi.org/10.1016/j.jddst.2023.104327

10. Nica MA, Anuța V, Nicolae CA, Popa L, Ghica MV, Cocoș FI, Dinu-Pîrvu CE (2024) Exploring Deep Eutectic Solvents as Pharmaceutical Excipients: Enhancing the Solubility of Ibuprofen and Mefenamic Acid. Pharmaceuticals (Basel) 17:1316. https://doi.org/10.3390/ph17101316

11. Ahamd S, Shmmon Ahmad, Anil Kumar, Abdul Hafeez, Rupinder Kaur (2018) Preparation and Evaluationof Ibuprofen Solid Dispersion Tablets with Improved Dissolution and Less Sticking Using Porous Calcium Silicate. J Pharm Pharmacol (Los Angel) 6:01–08. https://doi.org/10.13188/2327-204x.1000027

12. S. S. MrS (2021) Enhancement of Solubility Ibuprofen by Solid Dispersion Technique on Natural Mucilage. International Journal of Current Science Research and Review 04: https://doi.org/10.47191/ijcsrr/v4-i10-09

13. Al Masum MA, Sharmin F, Ashraful Islam SM, Reza MS (2012) Enhancement of solubility and dissolution characteristics of ibuprofen by solid dispersion technique. Dhaka University Journal of Pharmaceutical Sciences 11:. https://doi.org/10.3329/dujps.v11i1.12480

14. KAR A, AHMED AB (2017) ENHANCEMENT OF SOLUBILITY AND DISSOLUTION OF IBUPROFEN BY SOLID DISPERSION TECHNIQUE AND FORMULATION OF SUSTAINED RELEASE TABLETS CONTAINING THE OPTIMISED BATCH OF SOLID DISPERSION. Int J Curr Pharm Res. https://doi.org/10.22159/ijcpr.2017v9i5.22134

15. Chowdary KPR, Devi GSA, Susmitha K (2024) Enhancement of Solubility and Dissolution Rate of Ibuprofen: A Factorial Study Approach. In: Advanced Concepts in Pharmaceutical Research Vol. 5. B P International, pp 1–10

16. Singh S, Dash UN, Talukdar M (2020) Solubility enhancement and study of molecular interactions of poorly soluble ibuprofen in presence of urea, a hydrotropic agent. Mater Today Proc 30:246–253. https://doi.org/10.1016/j.matpr.2020.01.289

17. Kumar Patel S, Kumar D, Waghmode AP, SDhabale A (2011) Solubility enhancement of ibuprofen using hydrotropic agents. International Journal of Pharmacy and Life Sciences 2:542–545

18. Chowdary K, Devi G, Susmitha K (2024) Enhancement of Solubility and Dissolution Rate of Ibuprofen: A Factorial Study Approach. Focus on Microscopy 1–10. https://doi.org/10.34894/VQ1DJA

19. Wu YY, Zhao FQ, Ju XH (2014) A Comparison of the Accuracy of Semi-empirical PM3, PDDG and PM6 methods in Predicting Heats of Formation for Organic Compounds. J Mex Chem Soc 58:223–229. https://doi.org/10.29356/JMCS.V58I2.182

20. Stewart JJP (1989) Optimization of parameters for semiempirical methods II. Applications. J Comput Chem 10:221–264. https://doi.org/10.1002/JCC.540100209

21. Stewart JJP (1989) Optimization of parameters for semiempirical methods I. Method. J Comput Chem 10:209–220. https://doi.org/10.1002/JCC.540100208

22. Mane JY, Klobukowski M (2010) New parameterization of the PM3 method for monosaccharides. Chem Phys Lett 500:140–143. https://doi.org/10.1016/J.CPLETT.2010.09.069

23. Stewart JJP (2004) Optimization of parameters for semiempirical methods IV: Extension of MNDO, AM1 and PM3 to more main group elements. J Mol Model 10:155–164. https://doi.org/10.1007/S00894-004-0183-Z

24. Stewart JJP (1991) Optimization of parameters for semiempirical methods. III Extension of PM3 to Be, Mg, Zn, Ga, Ge, As, Se, Cd, In, Sn, Sb, Te, Hg, Tl, Pb, and Bi. J Comput Chem 12:320–341. https://doi.org/10.1002/JCC.540120306

25. Lin YS, Li G De, Mao SP, Chai J Da (2012) Long-Range Corrected Hybrid Density Functionals with Improved Dispersion Corrections. J Chem Theory Comput 9:263–272. https://doi.org/10.1021/CT300715S

26. Goerigk L, Grimme S (2011) A thorough benchmark of density functional methods for general main group thermochemistry, kinetics, and noncovalent interactions. Physical Chemistry Chemical Physics 13:6670–6688. https://doi.org/10.1039/C0CP02984J

27. Sharma D, Devi J, Sharma A, Sharma M, Raina M, Jamwal A, Roy TK (2025) Accuracy of DFT quadrature grids for the computation of quantum anharmonic vibrational spectroscopy. Vib Spectrosc 139:103810. https://doi.org/10.1016/J.VIBSPEC.2025.103810

28. Wavefun (2024) Basis Set FAQ. In: Wavefun Inc. https://downloads.wavefun.com/FAQ/BasisSetFAQ.html. Accessed 19 Jan 2024

29. Kestner NR, Combariza JE (1999) Basis Set Superposition Errors: Theory and Practice. In: Kenny BL, Donald BB (eds) Reviews in Computational Chemistry, 1st ed. John Wiley & Sons, Ltd, pp 99–132

30. Grimme S (2011) Density functional theory with London dispersion corrections. Wiley Interdiscip Rev Comput Mol Sci 1:211–228. https://doi.org/10.1002/WCMS.30

31. Grimme S, Antony J, Ehrlich S, Krieg H (2010) A consistent and accurate ab initio parametrization of density functional dispersion correction (DFT-D) for the 94 elements H-Pu. Journal of Chemical Physics 132:154104. https://doi.org/10.1063/1.3382344/926936

32. Oyegoke T, Aliyu A, Uzochuwu MI, Hassan Y (2024) Enhancing hydrogen sulphide removal efficiency: A DFT study on selected functionalized graphene-based materials. Carbon Trends 15:100362. https://doi.org/10.1016/J.CARTRE.2024.100362

33. Uzochukwu MI, Oyegoke T, Momoh RO, Isa MT, Shuwa SM, Jibril BY (2023) Computational insights into deep eutectic solvent design: Modeling interactions and thermodynamic feasibility using choline chloride & glycerol. Chemical Engineering Journal Advances 16:100564. https://doi.org/10.1016/J.CEJA.2023.100564

34. Muhammed UM, Oyegoke T (2025) Enhancing the Solubility of Metronidazole Using Deep Eutectic Solvents: A Computational Insight Into a Green Formulation Strategy. Res Sq 1:1–24. https://doi.org/10.21203/RS.3.RS-8106095/V1

35. NIST (2025) Propylene Glycol. In: NIST Chemistry WebBook, SRD 69. https://webbook.nist.gov/cgi/cbook.cgi?ID=C57556&Units=SI&Type=IR-SPEC&Index=1. Accessed 22 Nov 2025

36. Ayeni OI, Oyegoke T (2024) Computational insights into graphene-based materials for arsenic removal from wastewater: a hybrid quantum mechanical study. Discover Water 4:103. https://doi.org/10.1007/S43832-024-00160-3

37. Uzochukwu MI, Oyegoke T, Momoh RO, Isa MT, Shuwa SM, Jibril BY (2023) Computational insights into deep eutectic solvent design: Modeling interactions and thermodynamic feasibility using choline chloride & glycerol. Chemical Engineering Journal Advances 16:100564. https://doi.org/10.1016/J.CEJA.2023.100564

38. Santos CBR dos, Lobato CC, de Sousa MAC, Macêdo WJ da C, Carvalho JCT (2014) Molecular Modeling: Origin, Fundamental Concepts and Applications Using Structure-Activity Relationship and Quantitative Structure-Activity Relationship. Reviews in Theoretical Science 2:1–25. https://doi.org/10.1166/rits.2014.1016

39. Oyegoke T, Dabai FadimatuN, Adamu U, Baba YJ (2020) Quantum mechanics calculation of molybdenum and tungsten influence on the CrM-oxide catalyst acidity. Hittite Journal of Science & Engineering 7:297–311. https://doi.org/10.17350/HJSE19030000199

40. Olusola Ibraheem A, Toyese O (2025) DFT Fukui descriptor-based prediction of Arsenic adsorption on graphene. European Journal of Materials Science and Engineering 10:181–194. https://doi.org/10.36868/ejmse.2025.10.03.181

41. PubChem (2026) Ibuprofen, (+-)- | C13H18O2 | CID 3672 . In: PubChem Report. https://pubchem.ncbi.nlm.nih.gov/compound/Ibuprofen. Accessed 20 Mar 2026

42. Yalkowsky SH, He Y, Jain P (2016) Handbook of Aqueous Solubility Data. CRC Press, Boca Raton

43. Windholz M, Susan B, Lorraine YS, Margaret NF (1976) The Merck index : an encyclopedia of chemicals and drugs. Merck

44. PubChem (2026) Mefenamic Acid | C15H15NO2 | CID 4044. In: PubChem Report. https://pubchem.ncbi.nlm.nih.gov/compound/4044#section=Solubility. Accessed 20 Mar 2026

45. Húmpola P, Odetti HS, Albesa AG, Vicente JL (2013) Adsorption of phenols from different solvents on graphene: Semi-empirical quantum mechanical calculations. Adsorption Science and Technology 31:359–371. https://doi.org/10.1260/0263-6174.31.4.359

46. Zhang S, Hu X, Lu Q, Zhang J (2011) Density functional theory study of arsenic and selenium adsorption on the CaO (001) surface. Energy and Fuels 25:2932–2938. https://doi.org/10.1021/EF200043Q/SUPPL_FILE/EF200043Q_SI_001.PDF

47. Abbas A, Oyegoke T, Suleiman OS (2024) Molecular Simulation of Ibuprofen Adsorption on Pristine Graphene Membranes for Enhanced Industrial Effluent Treatment. In: 2024 NSChE E&R SG Mini-Conference and Workshop. NSChE Nigeria

48. Ibraheem Olusola A, Toyese O (2025) Insights on Metal Doped Graphene in the Adsorption of Arsenic via DFT Calculations. Chemistry Journal of Moldova In-press: https://doi.org/10.19261/cjm.2025.1264

49. Venkataramanan SSA, Anantharaj R, Venkataramanan SSA, Anantharaj R (2019) DFT Study on Interaction of Estrone and Imidazolium-Based Hydrophobic Ionic Liquids. In: Advances in Quantum Communication and Information. IntechOpen

50. Ghenaatian HR, Shakourian-Fard M, Alizadeh V, Kamath G (2022) DFT study of interaction of Palladium Pdn (n = 1–6) nanoparticles with deep eutectic solvents. J Mol Graph Model 110:108072. https://doi.org/10.1016/J.JMGM.2021.108072

51. Li G, Deng D, Chen Y, Shan H, Ai N (2014) Solubilities and thermodynamic properties of CO2 in choline-chloride based deep eutectic solvents. J Chem Thermodyn 75:58–62. https://doi.org/10.1016/J.JCT.2014.04.012

52. Cichowska-Kopczy´nska I, Kopczy´nska K, Nowosielski B, Warmí Nska D (2023) Deep Eutectic Solvents: Properties and Applications in CO2 Separation. Molecules 2023, Vol 28, Page 5293 28:5293. https://doi.org/10.3390/MOLECULES28145293

53. Haider MB, Jha D, Kumar R, Marriyappan Sivagnanam B (2020) Ternary hydrophobic deep eutectic solvents for carbon dioxide absorption. International Journal of Greenhouse Gas Control 92:102839. https://doi.org/10.1016/J.IJGGC.2019.102839

54. Oguche JE, Ameh AO, Bello TK, Maina NS (2023) Prospect of Deep Eutectic Solvents in Lactic Acid Production Process: A Review. Journal of Chemical Reviews 5:96–128. https://doi.org/10.22034/JCR.2023.349358.1203

55. Luo Y, Yin C, Ou L (2023) Recycling of waste lithium-ion batteries via a one-step process using a novel deep eutectic solvent. Science of The Total Environment 902:166095. https://doi.org/10.1016/J.SCITOTENV.2023.166095

56. Atkins PW (Peter W, De Paula J (2014) Physical chemistry : thermodynamics, structure, and change

57. Firme CL (2024) The electrostatic force applied to teaching organic chemistry in undergraduate classes. Quim Nova 47:e-20240014. https://doi.org/10.21577/0100-4042.20240014

58. Randol BM, Darwish SM (2023) Investigation of Coulomb's law and the nature of the electric charge. J Phys Commun 7:045001. https://doi.org/10.1088/2399-6528/ACCDB4

59. Traill D (2024) Electrostatic Attraction and Repulsion Explained and Modelled Mathematically Using Classical Physics—A Detailed Mechanism Based on Particle Wave Functions. Journal of Applied Mathematics and Physics 12:1050–1062. https://doi.org/10.4236/JAMP.2024.124065

60. Pauling L (1954) The dependence of bond energy on bond length. Journal of Physical Chemistry 58:662–666. https://doi.org/10.1021/J150518A015/ASSET/J150518A015.FP.PNG_V03

61. Zhao L, Zhi M, Frenking G (2022) The strength of a chemical bond. Int J Quantum Chem 122:26773. https://doi.org/10.1002/qua.26773

62. Smith JM (Joseph M, Van Ness HC (Hendrick C), Abbott MM (2005) Introduction to chemical engineering thermodynamics. McGraw-Hill

63. Metiu H (2006) Physical chemistry : thermodynamics. Taylor & Francis Group

Supplementary Files

This is a list of supplementary files associated with this preprint. Click to download.

- IBUMFAsupplementaryinfoREVISEDfinal.docx